Hydrogenic Impurity in Multi-layer Quantum Dots

Cheng-Ying Hsieh

德育醫護管理專科學校

Deh Yu College of Nursing and management, Keelung 204 , Taiwan

Abstract

The binding energies of hydrogenic impurity located at the center of a multi-layer quantum dot (MLQD) are studied within the framework of the effective-mass approximation. The MLQD consists of a spherical core (e.g. GaAs) and a coated spherical shell (e.g. $Ga_{1-x}Al_xAs$). The whole dot is then embedded inside a bulk material (e.g. $Ga_{1-y}Al_yAs$). The eigenfunctions of the impurity can be expressed in terms of Whittaker functions and Coulomb wave functions. For illustration, the ground state energy and binding energies are calculated as functions of the shell thickness, core radius, total dot radius and the potential heights. Our calculation shows that, as the dot radius approaches infinity, the ground state binding energy of a multi-layer or a single layer QD approaches 1Ry and behaves like that in a 3-dimensional free hydrogen atom. For very small dot radius, the ground state binding energy of the hydrogenic impurity located at the center of a MLQD behaves very different from that of a single layer QD. In contrast with 1Ry for a single

layer QD with finite potential height, the ground state binding energy of the impurity located at the center of a MLQD with finite shell and bulk potential barrier height approaches different limiting values from zero to 1Ry depending on the difference of the shell potential (V_2) and the bulk potential (V_3). For $V_2-1 \geqq V_3$, the electron tunnels to the bulk region and behaves like a free electron, and the ground state binding energy approaches zero for very small dot radius. For $V_2 \leqq V_3$, the electron tunnels to the shell region and the impurity atom behaves like a free hydrogen atom and the binding energy is equals to 1Ry. For $0<(V_2-V_3)<1$, the electron is able to stay either in the shell or in the bulk region and the binding energy is $1-(V_2-V_3)$.

PACS Number:63.20.Kr;71.38.+i

1. Introduction

The development and improvement of semiconductor growth techniques such as chemical vapor deposition (CVD), liquid-phase epitaxy (LPE) and molecular beam epitaxy (MBE), have led to the possibility of controlling material composition and of incorporating impurity on the electronic de Broglie scale[1-5]. Impurity states in various confined systems, such as quantum-well wires (QWWs) and quantum dots (QDs), have been a subject of extensive investigations in basic and applied research. Quasi-two-dimensional (quasi-2D) quantum wells (QWs) have been widely studied and applied to various semiconductor devices, such as high-electron-mobility transistors. Quasi-one-dimensional systems, such as quantum-well wires, are known to have the advantage of high mobility and suppression of carrier scattering.

Since Bastard's[6] pioneer works in the study of the binding energy of a hydrogenic impurity within an infinite potential-well structure, many theoretical works have been devoted to the study of the properties of impurity states in various confining systems[6-22]. The binding energy of the ground state of a hydrogenic impurity E_b in D dimensions is given by[23] $E_b=[2/(D-1)]^2$ Ry, where Ry is the effective Rydberg. In the 2-D case, the binding energy increases four times relative to the 3-D case, while in the 1-D case the increases is infinite. The binding energies for bound states of a hydrogenic impurity in a quantum-well wire with infinite[10] or finite[11] confining potential have also been studied. The binding energies for the bound states of a hydrogenic impurity in a quantum-well wire of GaAs-$Ga_{1-x}Al_xAs$ have been found to be 2-3 times larger than those of in comparable 2-D wells. The neutral acceptor binding energy was determined as a function of the GaAs quantum well width by using the photoluminescence and excitation spectra[12]. The ground state binding energy of the impurity located inside a QWW or a QD was calculated by many

authors[9-11,14,15,19-22]. All of the previous calculations showed the binding energy of the impurity atom in a quantum well depends prominently on the barrier height V_0 and the well(dot) size. The physical properties of electrons in quantum dots are very different from those in the bulk. As a consequence of the confinement, energy levels are discrete. The existence of these atomic-like state may be utilized in future laser where laser properties can be tailored by proper choices of well and barrier materials as well as sizes and shapes of the QDs. The change in impurity binding energies due to confinement effect has been observed in photoluminescence[12,24-26] and Raman-scattering[27,28] experiments on the impurities in the quantum wells. The study of the impurity states in quantum dots is of physics interest because specific properties of the impurity in lower-dimensional structures can be achieved easily by varying the radius of the quantum dot. The properties of an impurity atom in a quantum dot may appear to be unaffected by the boundary when the radius is very large. For an impurity in a QD with infinite confining potential, as the radius is reduced, the electron can move only in a smaller space and spends closer to the impurity ion. However, spatial confinement will cause the kinetic energy of the electron to increase due to the uncertainty principle and eventually may make the electron to overcome the attractive potential. Therefore, the total energy of the impurity may change from negative to positive for certain dot radius and finally diverges to infinity as the radius approaches zero. Moreover, the effective strength of the Coulomb interaction between the electron and the impurity atom depends on the geometric dimension of the system and is enhanced as the size of the system is reduced. Thus, the effective strength of the Coulomb interaction in QDs can be adjusted by varying the dot radius. On the contrary, dramatic changes in the binding energies may serve as a clear signal for changes in the effective dimension of QDs.

The first attempt to use more than a single quantum well was done by Chaudhuri[29], who used three quantum wells in his variational calculation of the ground-state energy of the donor electron with respect to the lowest subband level. P. Lane et al.[30] calculated the binding energies and probability distributions of shallow donor states in multiple-well GaAs-$Ga_xAl_{1-x}As$ heterostructure. Many authors[31-34] used colloidal chemistry techniques and wet chemistry to prepare the CdS/HgS/CdS multiple-well in which a shell of HgS is embedded in a CdS quantum dot, forming a "quantum-dot quantum well"(QDQW). The homogeneous absorption and fluorescence spectra of QDQW were investigated. Numerous studies on organic LEDs have used these structures as the emitting and charge transport species[35-37]. In this work we calculate the ground state binding energy of the hydrogenic impurity located at the center of the multi-layer quantum dot by using the effective-mass approximation. Our system is constructed as a core dot made of GaAs surrounded by a shell of $Ga_{1-x}Al_xAs$ and then embedded in the bulk of $Ga_{1-y}Al_yAs$. The polarization and image charge effects[38-40] may be significant in the multi-layer system if there is a large dielectric discontinuity between the dot and the surrounding medium. However, this is not the case for the GaAs-$Ga_{1-x}Al_xAs$ quantum system[21]; therefore these effects may be ignored safely in our calculation. The barrier height V between GaAs and $Ga_{1-x}Al_xAs$ can be obtained[41] as 0.8729x eV from a fixed ratio Q=0.7 of the band-gap discontinuity ΔE_g=1.247x eV. In this paper, the effective atomic units are used so that all energies are measured in the units of the effective Rydberg(Ry) and all distances are measured in the units of effective Bohr radius a_0^*. The Ry and a_0^* can be determined by $\frac{\mu e^4}{2\hbar^2\varepsilon^2}$ and $\frac{\varepsilon\hbar^2}{\mu e^2}$, where μ and ε are, respectively, the electronic effective mass and the dielectric constant of GaAs material and equal to

$0.067m_e$ and 13.18. Then the Ry and a_0^* are equal to 5.2 meV and 104 $\mathring{A}$, respectively. In this work, the effective-mass difference between GaAs and $Ga_{1-x}Al_xAs$ material has been ignored.

2. Theory

A. Hydrogenic impurity confined in the MLQD

Consider a hydrogenic impurity located at the center of a multi-layer spherical dot confined by spherical potential wells. The confining potential V_1 is assumed to be zero inside the dot (r<a); and V_2 inside the shell($a \leqq r < b$), V_3 outside the shell ($r \geqq b$), where a is the core radius and b is the total dot (core plus shell) radius, therefore b-a is the thickness of the shell. According to the effective-mass approximation, the Hamiltonian of the system can be written as

$$H = -\frac{\hbar^2}{2\mu}\nabla^2 - \frac{e^2}{\varepsilon r} + V(r)$$

where

$$V(r) = \begin{cases} 0, if\ r < a \\ V_2, if\ a \leq r < b \\ V_3, if\ r \geq b \end{cases}$$

and V(r) is the confining potential, μ and ε are the electronic effective mass and the dielectric constant of the material. The Schrödinger equation expressed in spherical coordinates (r, θ, φ)

$$H\Psi(r, \theta, \varphi) = E\Psi(r, \theta, \varphi) \qquad (1)$$

can be written as:

$$-\frac{\hbar^2}{2\mu}\left[\frac{\partial^2}{\partial r^2} + \frac{2}{r}\frac{\partial}{\partial r} + \frac{1}{r^2\sin\theta}\frac{\partial}{\partial\theta}\left(\sin\theta\frac{\partial}{\partial\theta}\right) + \frac{1}{r^2\sin^2\theta}\frac{\partial^2}{\partial\varphi^2}\right]\Psi - \frac{e^2}{\varepsilon r}\Psi + V(r)\Psi = E\Psi \qquad (2)$$

Separate $\Psi(r, \theta, \varphi)$ into a product of three terms $R(r)\Theta(\theta)\Phi(\varphi)$. Where

$\Theta(\theta)$ can be expressed in terms of the associated Legendre polynomial, and $\Phi(\varphi)=e^{im\varphi}$, m=0, ±1, ±2.... The equation for the radial part R(r) can be obtained as follows:

$$-\frac{\hbar^2}{2\mu}\left[\frac{\partial^2}{\partial r^2}+\frac{2}{r}\frac{\partial}{\partial r}-\frac{L(L+1)}{r^2}\right]R(r)-\frac{e^2}{\varepsilon r}R(r)+V(r)R(r)=ER(r) \qquad (3)$$

This equation can be solved in two different situations:

(I). For r < a , V(r)=0

Eq. (2) can be rewritten as

$$-\frac{\hbar^2}{2\mu}\left[\frac{\partial^2}{\partial r^2}+\frac{2}{r}\frac{\partial}{\partial r}-\frac{L(L+1)}{r^2}\right]R(r)-\frac{e^2}{\varepsilon r}R(r)=ER(r) \qquad (4)$$

As the electron is confined inside the core dot, the existence of positive energy bound states is possible, therefore, solutions of the Schrödinger equation can be studied in two regions:

(a). For negative-energy, E < 0.

Define $\alpha_{1a}^2=-\frac{8\mu E}{\hbar^2}>0, \xi=\alpha_{1a}r$ and $\lambda_1=\frac{2\mu e^2}{\varepsilon\hbar^2\alpha_{1a}}$, then Eq. (4) can be expressed as:

$$\frac{\partial^2 R}{\partial\xi^2}+\frac{2}{\xi}\frac{\partial R}{\partial\xi}+\left[-\frac{1}{4}+\frac{\lambda_1}{\xi}-\frac{L(L+1)}{\xi^2}\right]R=0 \qquad (5)$$

If we further write $R(\xi)=\xi^{-1}W(\xi)$, then Eq. (5) becomes

$$\frac{\partial^2 W}{\partial\xi^2}+\left[-\frac{1}{4}+\frac{\lambda_1}{\xi}+\frac{\frac{1}{4}-(L+\frac{1}{2})^2}{\xi^2}\right]W=0 \qquad (6)$$

Eq. (6) is the Whittaker equation[42,43] which has two linearly independent solutions :

$$W_{\lambda_1,L}(\xi)=e^{-\frac{\xi}{2}}\xi^{L+1}\Phi(L+1-\lambda_1,2L+2,\xi) \qquad (7a)$$

or

$$W_{\lambda_1,-L}(\xi) = e^{-\frac{\xi}{2}}\xi^{-L+1}\Phi(-L+1-\lambda_1,-2L+2,\xi) \tag{7b}$$

where Φ is the confluent hypergeometric function

$$\Phi(a,b,x) = 1+\frac{a}{b}\frac{x}{1}+\frac{a(a+1)}{b(b+1)}\frac{x^2}{2!}+\ldots+\frac{a(a+1)\ldots(a+k)}{b(b+1)\ldots(b+k)}\frac{x^k}{k!}+\ldots$$

$$=\sum_{k=0}^{\infty}\frac{(a)_k}{(b)_k}\frac{x^k}{k!}$$

The solution of Eq.(5) can be expressed as:

$$R(\xi) = \xi^{-1}W_{\lambda_1,L}(\xi) = e^{-\frac{\xi}{2}}\xi^{L}\Phi(L+1-\lambda_1,2L+2,\xi) \tag{8a}$$

or

$$R(\xi) = \xi^{-1}W_{\lambda_1,-L}(\xi) = e^{-\frac{\xi}{2}}\xi^{-L}\Phi(-L+1-\lambda_1,-2L+2,\xi) \tag{8b}$$

Since the wave function has to be finite everywhere, the solution of the radial part in the r < a region can be expressed as:

$$R_1(\alpha_{1a}r) = C_{1a}e^{-\frac{\alpha_{1a}r}{2}}(\alpha_{1a}r)^{L}\Phi(L+1-\lambda_1,2L+2,\alpha_{1a}r) \tag{9}$$

where C_{1a} is the normalization constant.

(b). For positive-energy, E > 0.

Define $\alpha_{1b}^2 = \frac{2\mu E}{\hbar^2} > 0$, $\xi = \alpha_{1b}r$ and $\beta_1 = -\frac{\mu e^2}{\varepsilon\hbar^2\alpha_{1b}}$, then Eq.(4) can be expressed as:

$$\frac{\partial^2 R}{\partial\xi^2}+\frac{2}{\xi}\frac{\partial R}{\partial\xi}+\left[1-\frac{2\beta_1}{\xi}-\frac{L(L+1)}{\xi^2}\right]R = 0 \tag{10}$$

If we further write $R(\xi) = \xi^{-1}F(\xi)$, then Eq.(10) becomes

$$\frac{\partial^2 F}{\partial\xi^2}+\left[1-\frac{2\beta_1}{\xi}-\frac{L(L+1)}{\xi^2}\right]F = 0 \tag{11}$$

Eq.(11) is the Coulomb wave equation[44] which has two linearly independent solutions $F_{\beta_1,L}(\xi)$ and $G_{\beta_1,L}(\xi)$, where

$$F_{\beta_1,L}(\xi)=\xi^{L+1}\Phi_{\beta_1,L}(\xi).,\qquad (12a)$$

$$G_{\beta_1,L}(\xi)=F_{\beta_1,L}(\xi)\left[\ln(2\xi)+\frac{q_L(\beta_1)}{p_L(\beta_1)}\right]+\theta_{\beta_1,L}(\xi)\qquad (12b)$$

and

$$\Phi_{\beta_1,L}(\xi)=\sum_{k=L+1}^{\infty}A_k^L(\beta_1)\xi^{k-L-1}$$

The recurrence relation can be expresséd as:

$$A_{L+1}^L(\beta_1)=1$$

$$A_{L+2}^L(\beta_1)=\frac{\beta_1}{L+1}$$

$$A_k^L(\beta_1)=\frac{2\beta_1A_{k-1}^L(\beta_1)-A_{k-2}^L(\beta_1)}{(k+L)(k-L-1)}\quad for\ k>L+2$$

$G_{\beta_1,L}(\xi)$ is singular at $\xi=0$, hence the wave function of the radial part in the region E > 0 can be expressed as

$$R_1(\alpha_{1b}r)=C_{1b}\sum_{k=L+1}^{\infty}A_k^L(\beta_1)(\alpha_{1b}r)^{k-1}\qquad (13)$$

where C_{1b} is the normalization constant.

(c). For zero energy E=0.

Substituting E=0 into Eq.(4) , one obtains:

$$r^2\frac{\partial^2R(r)}{\partial r^2}+2r\frac{\partial R(r)}{\partial r}+\left[-L(L+1)+\frac{2\mu e^2}{\varepsilon\hbar^2}r\right]R(r)=0\qquad (14)$$

Comparing with the modified Bessel equation

$$r^2\frac{\partial^2u(r)}{\partial r^2}+(1-2\omega)r\frac{\partial u(r)}{\partial r}+(\omega^2-\nu^2\gamma^2+\alpha^2\gamma^2r^{2\gamma})u(r)=0\qquad (15)$$

If we set ω=-1/2, γ=1/2, ν=2L+1, and $\alpha_{1c}^2=\frac{8\mu e^2}{\varepsilon\hbar^2}$, then the solution of Eq.(15) can be expressed as :

$$u(\alpha_{1c}r) = r^{\omega}\left[C_{1c}J_{\nu}(\alpha_{1c}r^{\gamma}) + C_{1c}N_{\nu}(\alpha_{1c}r^{\gamma})\right]$$

where $J_{\nu}(\alpha_{1c}r^{\gamma})$ is Bessel function and $N_{\nu}(\alpha_{1c}r^{\gamma})$ is Neumann function. Since the radial function must be finite for L=0, therefore, the wave function of radial part can be written as

$$R_1(\alpha_{1c}r) = C_{1c}r^{-\frac{1}{2}}J_{2L+1}\left(\sqrt{\frac{8\mu e^2}{\varepsilon\hbar^2}}r^{\frac{1}{2}}\right) \qquad (16)$$

(II). For $a \leqq r < b$, $V(r)=V_2$

The differential equation for the radial part R(r) can be expressed as:

$$-\frac{\hbar^2}{2\mu}\left[\frac{\partial^2}{\partial r^2}+\frac{2}{r}\frac{\partial}{\partial r}-\frac{L(L+1)}{r^2}\right]R(r)-\frac{e^2}{\varepsilon r}R(r)+V_2R(r)=ER(r) \qquad (17)$$

Define $\alpha_2^2 = -\frac{8\mu(E-V_2)}{\hbar^2} > 0$, $\xi = \alpha_2 r$, $\lambda_2 = \frac{2\mu e^2}{\varepsilon\hbar^2\alpha_2}$ and $R(\xi) = \xi^{-1}W(\xi)$, then Eq.(17) can be rewritten as:

$$\frac{\partial^2 W}{\partial\xi^2}+\left[-\frac{1}{4}+\frac{\lambda_2}{\xi}+\frac{\frac{1}{4}-(L+\frac{1}{2})^2}{\xi^2}\right]W=0 \qquad (18)$$

This is the Whittaker equation. Thus, the solution can be written as:

$$\begin{aligned}R_2(\alpha_2 r) &= C_{21}e^{-\frac{\alpha_2 r}{2}}(\alpha_2 r)^L\Phi(L+1-\lambda_2,2L+2,\alpha_2 r)\\ &+c_{22}e^{-\frac{\alpha_2 r}{2}}(\alpha_2 r)^L\{\Phi(L+1-\lambda_2,2L+2,\alpha_2 r)\ln(\alpha_2 r)\\ &+\sum_{k=0}^{\infty}\frac{(L+1-\lambda_2)_k}{(2L+2)_k}\frac{(\alpha_2 r)^k}{k!}\times\left[\phi(L+1-\lambda_2+k)-\phi(2L+2+k)-\phi(1+k)\right]\\ &+\frac{\Gamma(2L+1)\Gamma(2L+2)\Gamma(-L-\lambda_2)(-1)^{2L+2}}{\Gamma(L+1-\lambda_2)}\times\sum_{k=0}^{2L}\frac{(-L-\lambda_2)_k}{(-2L)_k}\frac{(\alpha_2 r)^{k-2L-1}}{k!}\Bigg\}\end{aligned} \qquad (19)$$

where C_{21}, C_{22} are normalization constants.

(Ⅲ). For $r \geqq b$, $V(r)=V_3$

The differential equation for the radial part R(r) can be expressed as:

$$-\frac{\hbar^2}{2\mu}\left[\frac{\partial^2}{\partial r^2}+\frac{2}{r}\frac{\partial}{\partial r}-\frac{L(L+1)}{r^2}\right]R(r)-\frac{e^2}{\varepsilon r}R(r)+V_3R(r)=ER(r) \qquad (20)$$

Define $\alpha_3^2=-\frac{8\mu(E-V_3)}{\hbar^2}>0$, $\xi=\alpha_3 r$, $\lambda_3=\frac{2\mu e^2}{\varepsilon\hbar^2\alpha_3}$, and $R(\xi)=\xi^{-1}W(\xi)$, then Eq.(20) becomes

$$\frac{\partial^2 W}{\partial\xi^2}+\left[-\frac{1}{4}+\frac{\lambda_3}{\xi}+\frac{\frac{1}{4}-(L+\frac{1}{2})^2}{\xi^2}\right]W=0 \qquad (21)$$

This is the Whittaker equation. The Whittaker functions expressed in Eq.(7a) and Eq.(7b) are not well behaved as ξ becomes very large, we thus turn to use the integral representation of Whittaker function

$$W_{\lambda_3,L}(\xi)=C_3e^{-\frac{\xi}{2}}\xi^{\lambda_3}\int_0^\infty e^{-t}t^{-\lambda_3+L}(1+\frac{t}{\xi})^{\lambda_3+L}dt \qquad (22)$$

in our calculation. Hence the radial part wave function in the $r>b$ region can be written as

$$R_3(\alpha_3 r)=C_3e^{-\frac{\alpha_3 r}{2}}(\alpha_3 r)^{\lambda_3-1}\int_0^\infty e^{-t}t^{-\lambda_3+L}(1+\frac{t}{\alpha_3 r})^{\lambda_3+L}dt \qquad (23)$$

The boundary conditions require:

$$\frac{R_1'(\alpha_1 a)}{R_1(\alpha_1 a)}=\frac{R_2'(\alpha_2 a)}{R_2(\alpha_2 a)} \qquad (24)$$

$$\frac{R_2'(\alpha_2 b)}{R_2(\alpha_2 b)}=\frac{R_3'(\alpha_3 b)}{R_3(\alpha_3 b)} \qquad (25)$$

Using above two equations, one can obtain the eigenvalue E.

B. electron confined in the MLQD

The Hamiltonian of an electron confined in the MLQD can be written

as:

$$H = -\frac{\hbar^2}{2\mu}\nabla^2 + V(r) \tag{26}$$

where

$$V(r) = \begin{cases} 0\ , if\ r < a \\ V_2\ , if\ a \le r < b \\ V_3\ , if\ r \ge b \end{cases}$$

Schrödinger equation for the radial part R(r) can be expressed in spherical coordinate as:

$$r^2\frac{\partial^2 R(r)}{\partial r^2} + 2r\frac{\partial R(r)}{\partial r} + \left[-L(L+1) - \frac{2\mu V(r)}{\hbar^2}r^2\right]R(r) = -\frac{2\mu}{\hbar^2}Er^2R(r) \tag{27}$$

(Ⅰ). For r＜a , V(r)=0

The Eq (27) can be written as

$$r^2\frac{\partial^2 R(r)}{\partial r^2} + 2r\frac{\partial R(r)}{\partial r} + \left[-L(L+1) + \frac{2\mu E}{\hbar^2}r^2\right]R(r) = 0 \tag{28}$$

Comparing with the modified Bessel equation (Eq.(15)), the wave function of the radial part can be expressed as

$$R_1(r) = C_1 r^{-\frac{1}{2}} J_{L+\frac{1}{2}}\left(\sqrt{\frac{2\mu E}{\hbar^2}}r\right) \tag{29}$$

(Ⅱ). For a≦r＜b, V(r)=V_2

Set $\alpha_2^2 = -\frac{8\mu(E-V_2)}{\hbar^2} > 0$, $\xi = \alpha_2 r$, and R(ξ)= ξ^{-1}W(ξ), then Eq.(27) becomes

$$\frac{\partial^2 W}{\partial \xi^2} + \left[-\frac{1}{4} + \frac{\frac{1}{4} - (L+\frac{1}{2})^2}{\xi^2}\right]W = 0 \tag{30}$$

This is the Whittaker equation. Thus, the solution of the system can be written as

$$R_2(\alpha_2 r) = C_{21} e^{-\frac{\alpha_2 r}{2}} (\alpha_2 r)^L \Phi(L+1, 2L+2, \alpha_2 r)$$

$$+ C_{22} e^{-\frac{\alpha_2 r}{2}} (\alpha_2 r)^{-L-1} \Phi(-L, -2L, \alpha_2 r) \qquad (31)$$

(Ⅲ). For $r \geqq b$, $V(r)=V_3$.

Let $\alpha_3^2 = -\frac{8\mu(E-V_3)}{\hbar^2} > 0$, $\xi = \alpha_3 r$, and $R(\xi) = \xi^{-1} W(\xi)$. Then Eq. (27) becomes

$$\frac{\partial^2 W}{\partial \xi^2} + \left[-\frac{1}{4} + \frac{\frac{1}{4} - (L+\frac{1}{2})^2}{\xi^2} \right] W = 0 \qquad (32)$$

which is the Whittaker equation, and the solution of the system can be written as

$$R_3(\alpha_3 r) = C_3 e^{-\frac{\alpha_3 r}{2}} (\alpha_3 r)^{-1} \int_0^\infty e^{-t} t^L (1 + \frac{t}{\alpha_3 r})^L dt \qquad (33)$$

Using boundary conditions

$$\frac{R_1'(\alpha_1 a)}{R_1(\alpha_1 a)} = \frac{R_2'(\alpha_2 a)}{R_2(\alpha_2 a)} \qquad (34)$$

$$\frac{R_2'(\alpha_2 b)}{R_2(\alpha_2 b)} = \frac{R_3'(\alpha_3 b)}{R_3(\alpha_3 b)} \qquad (35)$$

one can obtain the eigenvalue E.

3. Results and discussions

The binding energy E_b of the impurity is defined as the difference between the electron energy with and without the binding of the impurity atom[6, 10, 11, 14, 15, 19-22, 29], i.e.

$$E_b = E_e - E_i$$

where E_i and E_e represent the state energies of electron in multi-layer

QD with and without impurity. In this work, we only calculate the ground state binding energy of a hydrogenic impurity located at the center of a multi-layer quantum dot for different confining potential energies and radius of the core and total dot. The excited state binding energies can be easily obtained in a similar treatment. To make a comparison, we first set $V_2=V_3=V$ which is equivalent to consider the case of a single layer quantum dot. For a single layer quantum dot with very large dot radius, the impurity behaves just like a 3-dimensional free hydrogen atom, thus its binding energy will approach the 3-dimensional value 1Ry. If the dot radius decreases, the confinement effect enhances the binding energy more prominently. Thus, the binding energy of the impurity increases monotonically with the dot radius. However, as the dot radius is further decreased, the state energy of the impurity may become higher than the confining barrier. In the meanwhile, the kinetic energy of the confined electron becomes larger by uncertainty principle and thus increases the probability of the electron leaking outside the well. The electron behaves like a 3-dimensional electron after certain characteristic dot radius and is only weakly perturbed by the potential well. Therefore, the binding energy resumes 1Ry again.

Figs. 1a and 1b show the calculated ground state energy and the binding energy of a hydrogenic impurity located at the center of a MLQD with $V_2=V_3=V$ as a function of dot radius for four different potential barriers. For infinite potential barrier, as the dot radius decreases from infinite to zero, the impurity energy increases monotonically from -1Ry to infinite. On the contrary, the binding energy of the impurity approaches 1Ry as the radius becomes very large and diverges to infinite as the dot radius shrinks to zero. According to Fig. 1, one can see that instead of the divergence of the energy for zero dot radius QD with an infinite potential, the ground state energy of the impurity located at

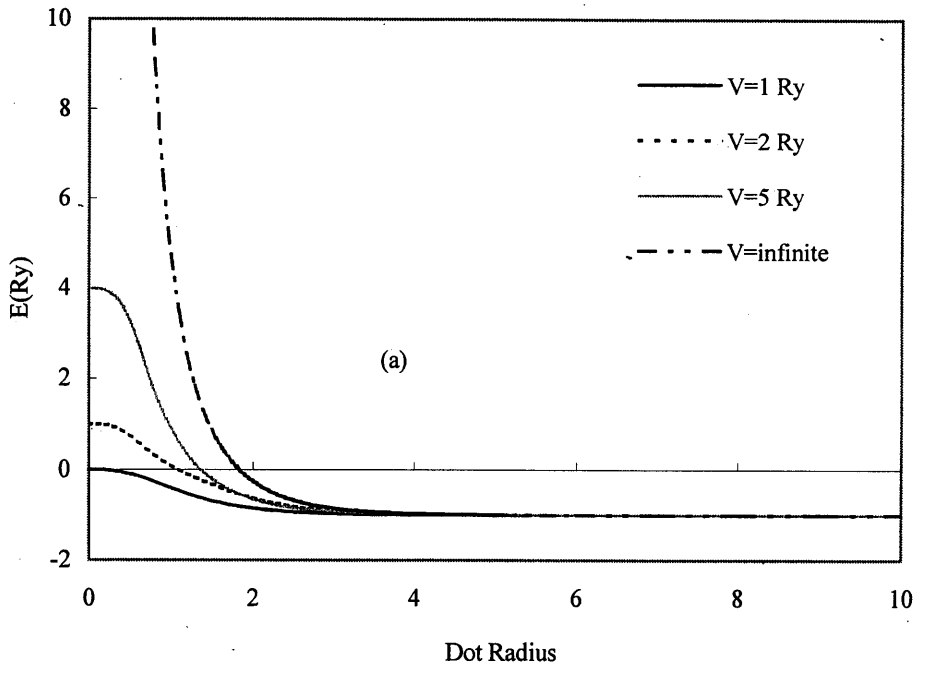

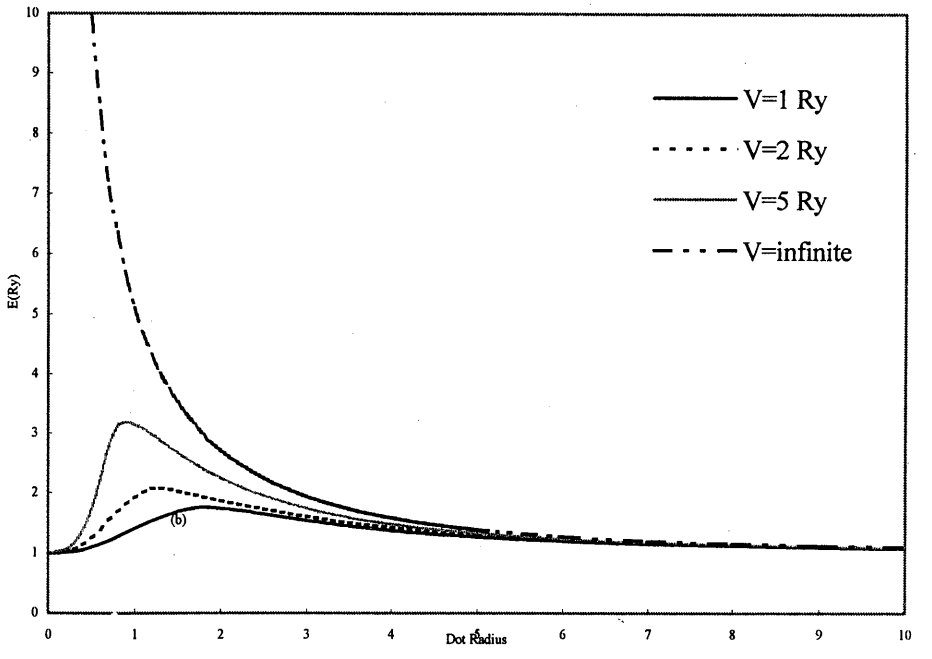

Fig. 1 (a) The ground state energy and (b) the ground state binding energy of a hydrogenic impurity in single layer QD as a function of dot radius with potential barrier V=1Ry , 2Ry, 5Ry and ∞ Ry respectively.

the center of a MLQD ($V_2=V_3=V$) with a finite height potential barrier approaches (V-1)Ry as the dot radius becomes zero. For finite potential barrier, our calculated results show, as the dot radius decreases from infinite to zero, the binding energy increases monotonically from 1Ry to a maximum value for a dot radius (a_m)~1.5a_0^*, then decreases monotonically to 1Ry finally. This is consistent with the previous result[14] Therefore, our results for the multi-layer QD can be successfully reduced to the single layer QD case as we set $V_2=V_3$.

Now let us come back to the case of the multi-layer quantum dot ($V_2 \neq V_3$). Fig. 2a shows the ground state energies of an electron in a multi-layer QD without impurity with V_2=5Ry but various V_3. Fig. 2b shows the ground state energies of an electron in a multi-layer QD without impurity with V_3=5Ry but various V_2. One can see that the ground state energies approach VRy as the dot radius approaches zero, where $V=V_2$ if $V_2<V_3$, and $V=V_3$ if $V_3<V_2$. This means that the electron leaks out, as the core radius reduces to some characteristic value, and finally the electron stays in the region with a smaller potential barrier in the multi-layer QD. Fig. 3a shows the ground state energy of an impurity located in a multi-layer quantum dot with V_3=5Ry , b=24a_0^* but various potential barrier V_2. According to Fig. 3a, as the core radius approaches infinite, the ground state energy approaches -1Ry, which is the same as the result of single layer QD. The ground state energy increases as the core radius decreases, and it attains to a characteristic value E_{i0} as the radius reduces to zero. In the case of a single layer QD, the E_{i0} is equal to VRy. In the case of a multi-layer QD, the value of E_{i0} depends on the value of (V_2-V_3) and the shell thickness b-a. As the core radius a reduces to zero, the electron leaks out of the dot core and tunnels to the shell region ($a \leqq r < b$) for $V_2-1<V_3$ or to the bulk region ($r \geqq b$) for $V_2-1>V_3$. If the electron tunnels to the shell region with a large shell thickness,

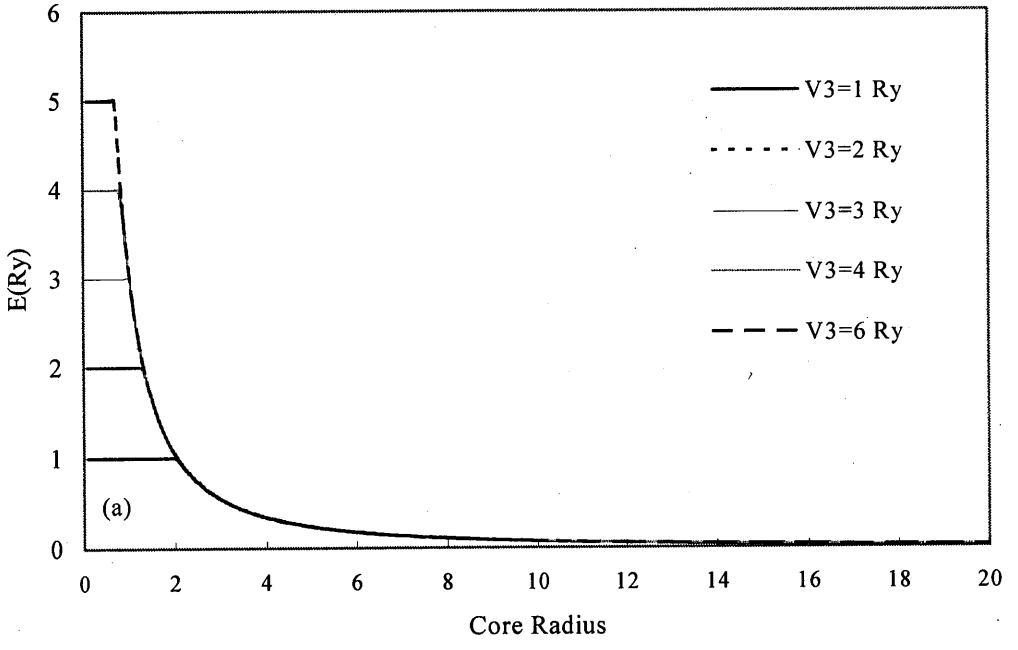

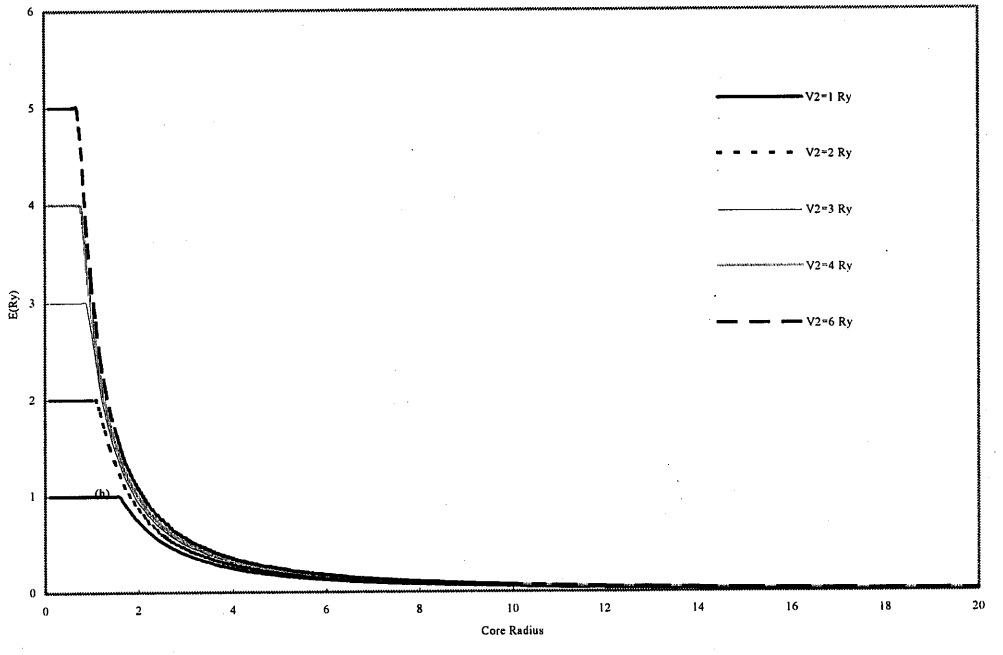

Fig. 2 The ground state energy of electron in multi-layer QD without impurity as a function of core radius for b=24a_0^*, (a) the shell potential V_2=5Ry, and V_3=1Ry, 2Ry, 3Ry, 4Ry, ∞Ry, (b) the bulk potential V_3=5Ry, and shell potential V_2=1Ry, 2Ry, 3Ry, 4Ry, ∞Ry, respectively.

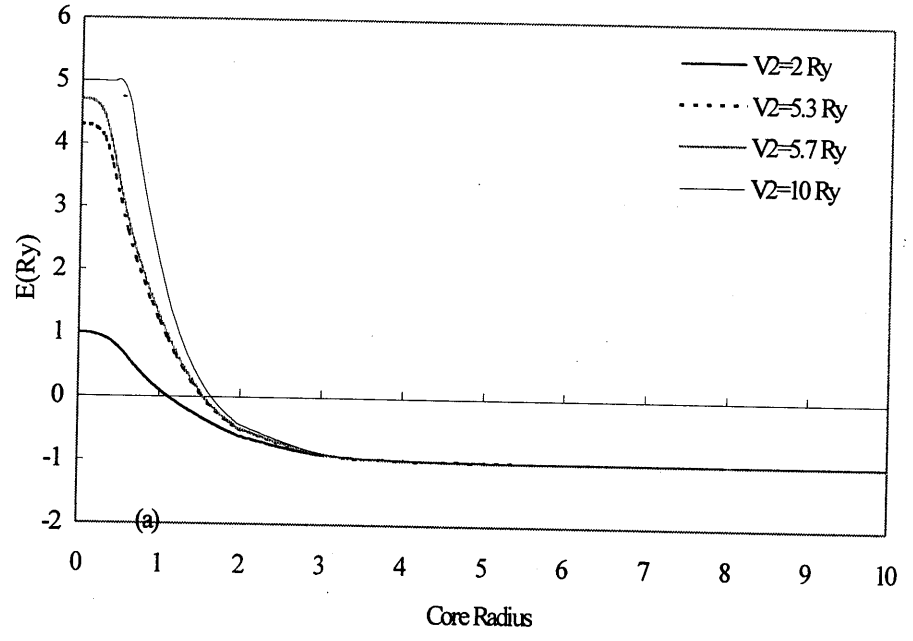

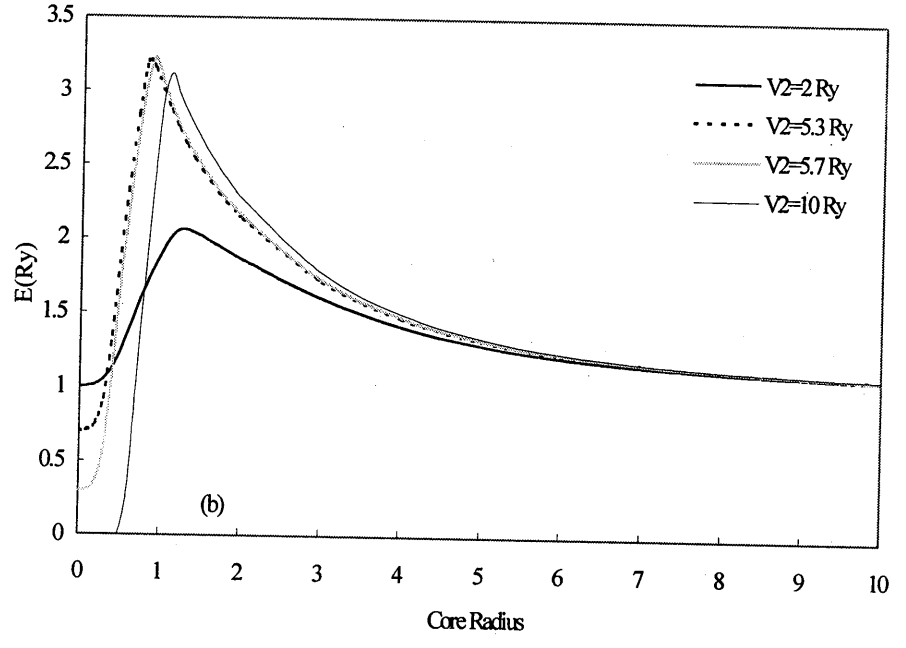

Fig. 3 (a) The ground state energy and (b) the ground state binding energy of electron in multi-layer QD with impurity as a function of core radius for b=24 a_0^*, the shell potential V_3=5Ry, and V_2=2Ry, 5.3Ry, 5.7Ry, 10Ry, respectively.

the ground state energy (E_{i0}) of electron becomes (V_2-1). It behaves like the case of single layer quantum dot with potential barrier equals V_2. If the electron tunnels to the bulk region with a large shell thickness, then the ground state energy of the electron becomes V_3. In this case, the electron behaves just like a free electron in the bulk without the binding of the impurity. The above results can be summarized as follows:

(1). for $V_2-1 \geqq V_3$, the electron tunnels to the bulk region as the core radius reduces to zero, and the ground state energy of the electron is V_3 for both cases with or without the impurity atom. And the binding energy of the electron is zero for very small core radius.

(2). for $V_2 \leqq V_3$, the electron tunnels to the shell region as the core radius reduces to zero. The ground state energy equals V_2 for an electron without the impurity binding and equals V_2-1 for an electron with the impurity binding. The binding energy is then equals to 1Ry and the system behaves like a free hydrogen atom in the shell region.

(3). $0<(V_2-V_3)<1$, the electron without the impurity binding tunnels to the bulk region as the core radius reduces to zero and the ground state energy is V_3, while that with the impurity binding tunnels to the shell region and the ground state energy is V_2-1. Therefore, the binding energy is 1-(V_2-V_3), and the electron can be in either the shell region or the bulk region. This result can be obtained also by the following consideration. For the case of $0<(V_2-V_3)<1$, as the core radius reduces to zero, the electron may tunnel to bulk region or shell region depending on the value of (V_2-V_3). As the core radius reduces to zero, for $V_2 \leqq V_3$, the relative probability of electron tunneling to the shell region is 100%, while for $(V_2-1) \geqq V_3$, the relative probability of electron tunneling to the bulk region is 100%. As the value of (V_2-V_3) increases from 0Ry to 1Ry, the relative probability of electron tunneling to the shell region decreases from 100% to 0% and the relative probability

of electron tunneling to the bulk region increases from 0% to 100%. For $0<(V_2-V_3)<1$, the relative probability of electron tunneling to bulk region can be set as

$$\frac{(V_2-V_3)Ry}{1\ Ry}=(V_2-V_3)\equiv p_b$$

and the relative probability of electron tunneling to shell region can be set as

$$1-\frac{(V_2-V_3)Ry}{1\ Ry}=1-(V_2-V_3)\equiv p_s$$

Thus as the core radius approaches zero the binding energy can be defined as

E_{b0}= (binding energy of the electron in the shell region)$\times P_s$+ (binding energy of the electron in the bulk region)$\times P_b$

= 1Ry $\times$ P_s + 0Ry $\times$ P_b

= P_s Ry = 1-(V_2-V_3) Ry

which is consistent with our calculated results as shown in Fig. 3b. Fig. 3b shows the ground state binding energy of a hydrogenic impurity in multi-layer QD as a function of core radius for b=24a_0^*, and the shell potential V_3=5Ry, V_2=2Ry, 5.3Ry, 5.7Ry, 10Ry respectively. Our calculated results show, as the core radius is decreased from infinite to zero, the ground state binding energy increases from 1Ry monotonically until it attains a maximum value, then, it decreases to a limit value which is agreement with the above discussion. As the ground state binding energy is concerned, the results of a multi-layer QD is similar to that of a single layer QD for large dot radius and is very different for small dot radius. In the single layer QD, the E_{b0} is 1Ry for any potential barrier height. However, in the multi-layer QD, the E_{b0} may change from zero to 1Ry by varying the difference between shell potential height and bulk potential height. And the position of the electron can be adjusted by varying the shell and bulk potential height as the core radius reduces

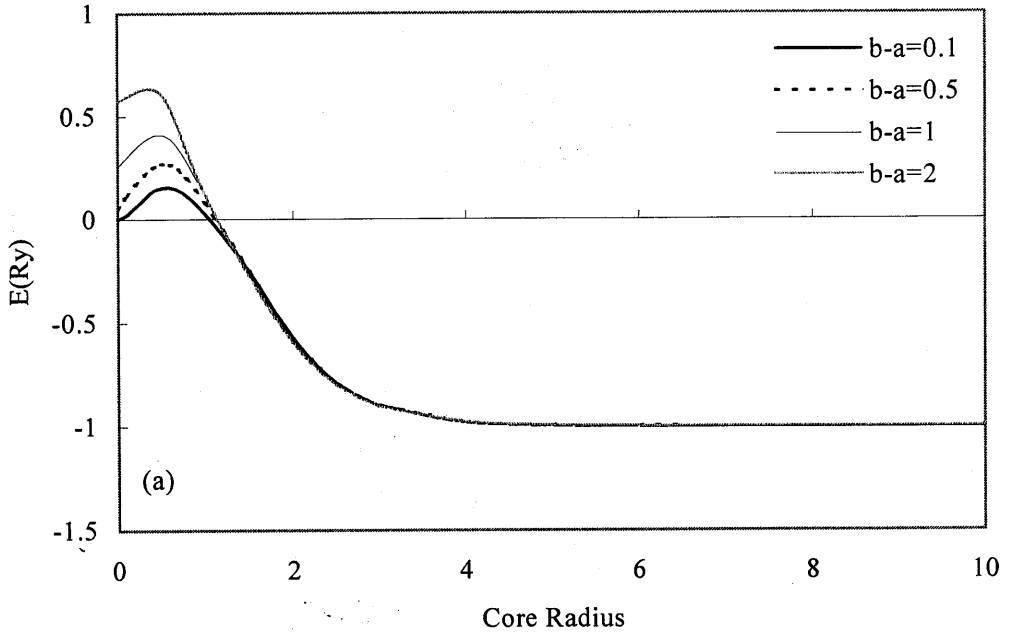

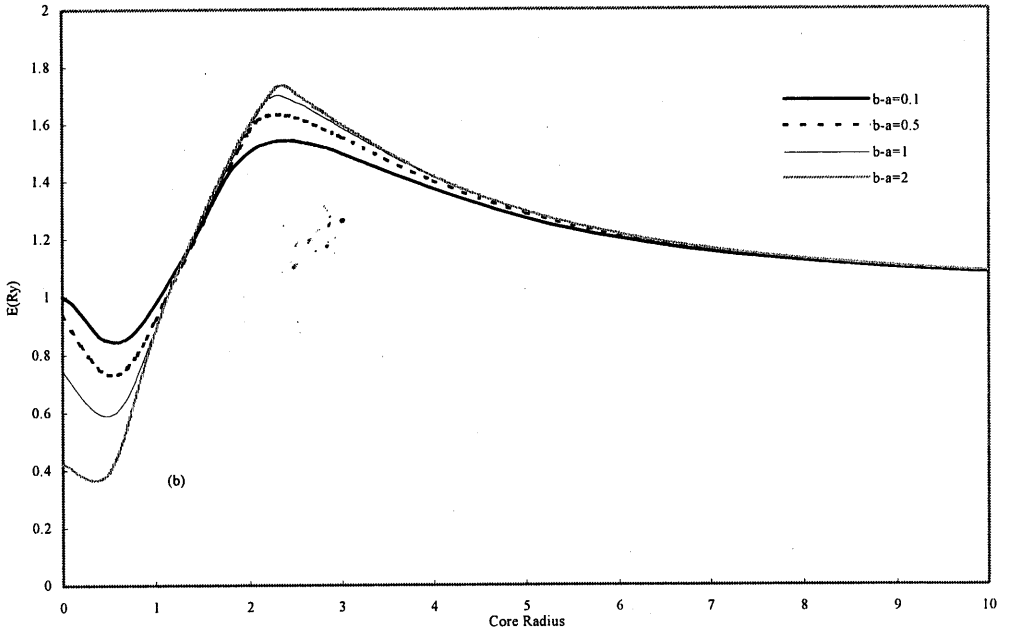

Fig. 4 (a) The ground state energy and (b) the ground state binding energy of a hydrogenic impurity in multi-layer QD as a function of core radius with V_2=2Ry and V_3=1Ry for various thickness of shell (b-a)=0.1a_0^*, 0.5a_0^*, 1a_0^*, 2a_0^*, respectively.

to zero.

Fig. 4a and 4b show the ground state energy and binding energy of a hydrogenic impurity in multi-layer QD as a function of core radius with V_2=2Ry and V_3=1Ry for various shell thickness (b-a)=0.1, 0.5, 1, $2a_0^*$ respectively. For large core radius, the impurity inside the multi-layer QD behaves like a free hydrogen atom even though the shell thickness is different. As the core radius decreases, the energy increases monotonically until it attains a maximum value, and then decreases monotonically to certain limiting value as the core radius approaches zero as shown in Fig. 4a. The limiting value depends on the shell thickness. This is because the tunneling probability of the electron depends on the shell thickness for small core radius. As the thickness of shell decreases, and then decreases monotonically to certain limiting value as the core radius approaches zero as shown in Fig. 4a. The limiting value depends on the shell thickness. This is because the tunneling probability of the electron depends on the shell thickness for small core radius. As the thickness of shell decreases, the probability of tunneling to bulk region increases and the maximum value of the state energy decreases. One can note from Fig. 4a, that the probability of electron tunneling increases as the shell thickness decreases. In Fig. 4b, one can also note that the thickness of shell affects the binding energy for small core radius.

Figs. 5a and 5b show the ground state energy and binding energy of a hydrogenic impurity in a multi-layer QD as a function of core radius with V_2=2Ry and the shell thickness is kept as (b-a)=$1a_0^*$ for various V_3. For small radius, the effect of the height of bulk potential barrier is more important. In Fig. 5a, one can note that the maximum value of the state energy for the case of V_3=1.5Ry is larger than that of V_3=1Ry. Thus the height of the bulk potential barrier influences the electron tunneling.

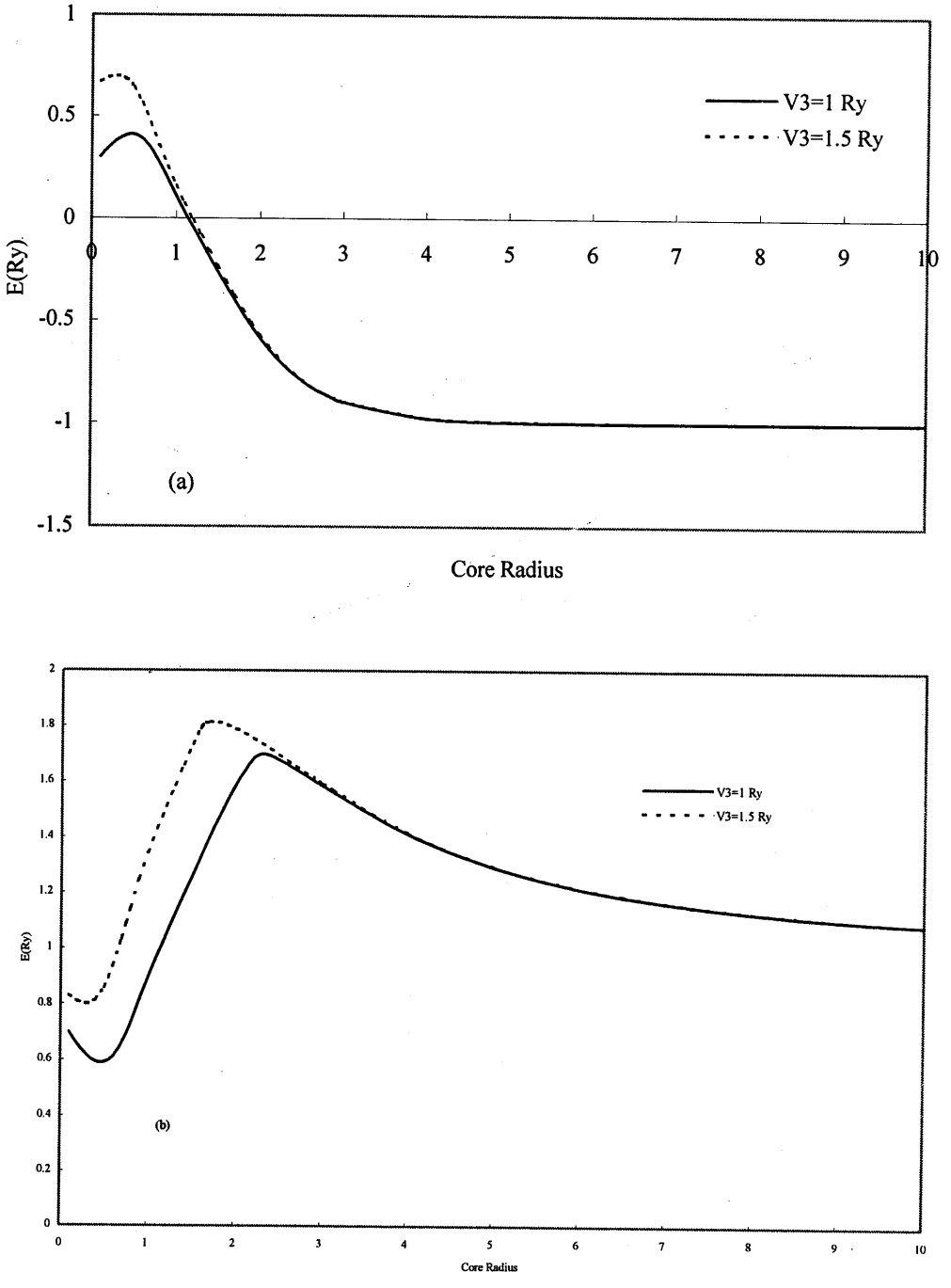

Fig. 5 (a) The ground state energy and (b) the ground state binding energy of a hydrogenic impurity in multi-layer QD as a function of core radius with V_2=2Ry and (b-a)=1a_0^* for various V_3=1Ry, 1.5Ry, respectively.

As shown in Fig. 5b, the height of the bulk potential barrier affects the binding energy for small core radius. Fig. 6 shows the binding energy of a hydrogenic impurity in the multi-layer QD as a function of total dot radius with V_2=5Ry and a=1 a_0^* for various V_3. The binding energy decreases monotonically as the total dot radius is decreased as the core radius is kept constant. Fig. 7a shows the binding energy of a hydrogenic impurity in the multi-layer QD as a function of core radius with V_2=3Ry and b=5 a_0^* for various V_3. As the core radius approaches 5 a_0^* (the shell thickness approaches zero), the effect of multi-layer ($V_2 \neq V_3$) can be observed on the boundary. In Fig. 7a, the binding energies of V_3=1Ry and V_3=2Ry do

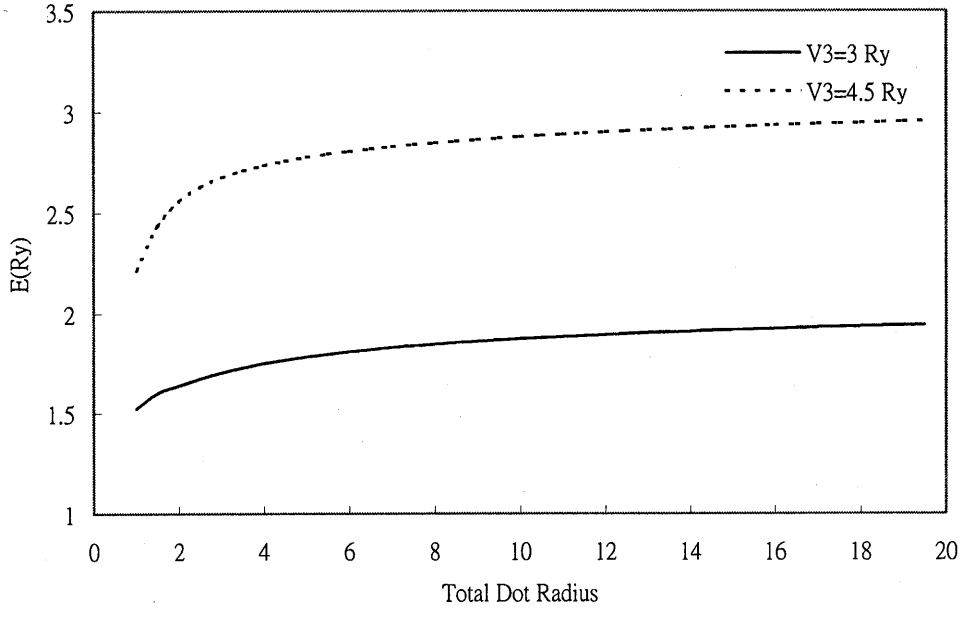

Fig. 6 The ground state binding energy of a hydrogenic impurity in multi-layer QD as a function of total dot radius with V_2=5Ry and a=1 a_0^* for various V_3=3Ry, 4.5Ry, respectively.

not approach 0Ry as the core radius reduces to zero. This is because that the shell radius is not large enough, the electron tunneling to bulk region is now only slightly interacted by the impurity. Fig. 7b shows the binding energy of a hydrogenic impurity in the multi-layer QD as a function of core radius with V_3=3Ry and b=5 a_0^* for various V_2. Comparing Fig. 7a

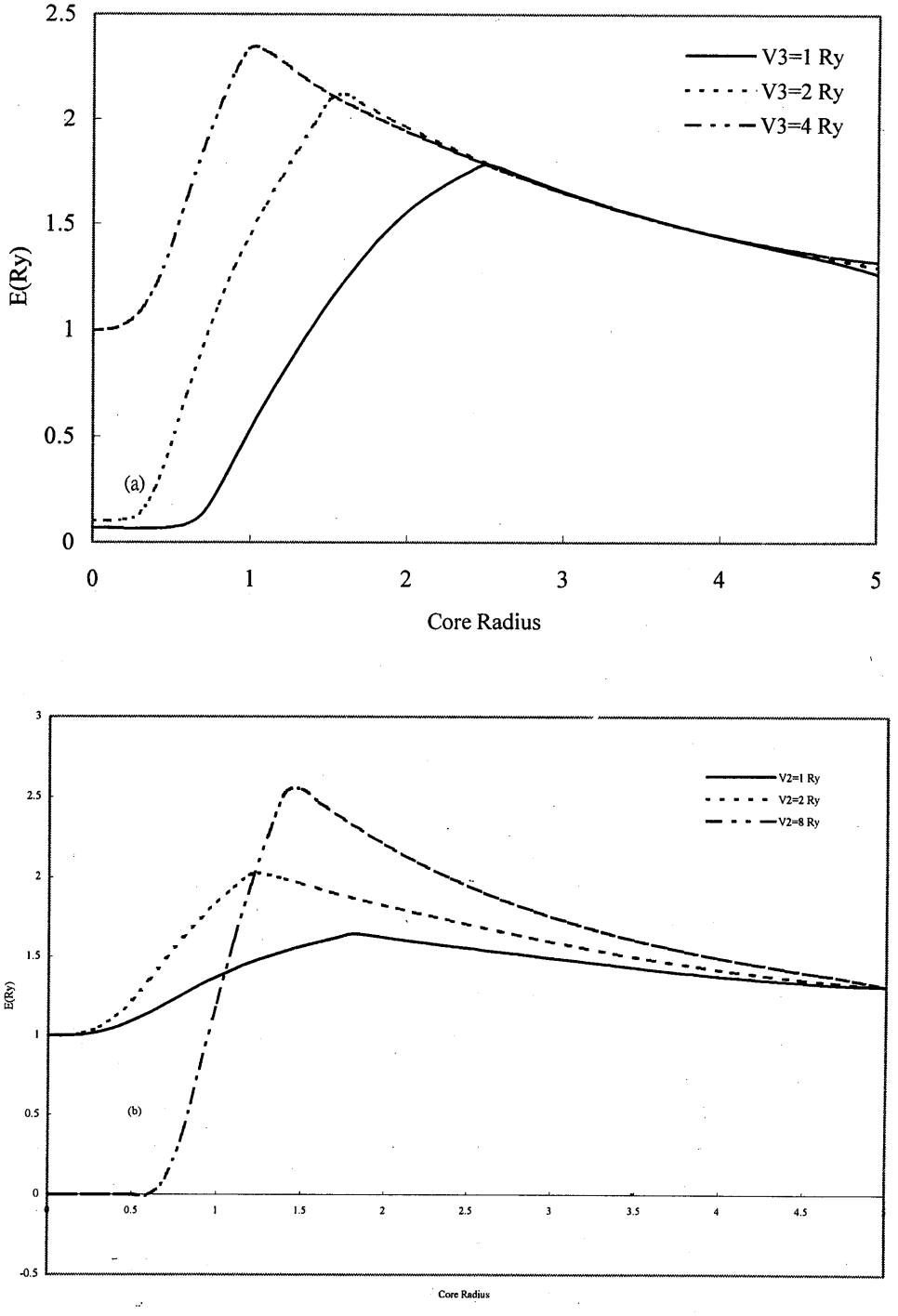

Fig. 7 The ground state binding energy of a hydrogenic impurity in multi-layer QD as a function of core radius with (a) V_2=3Ry and b=5a_0^* for various V_3=1Ry, 2Ry, 4Ry, (b) V_3=3Ry and b=5a_0^* for various V_2=1Ry, 2Ry, 8Ry, respectively.

with Fig. 7b, one can note that the effect of the barrier height of the shell potential is more important than the barrier height of the bulk potential on the binding energy. In Fig. 7b, the binding energy approaches correct limits. Comparing the binding energy curve of V_2=8Ry, V_3=3Ry in Fig. 7b with that of V_2=3Ry, V_3=1Ry in Fig. 7a, one can observe that the binding energies for both curves approach different values as the core radius reduces to zero. This is because the different values of (V_2-V_3) involved in both cases.

4. Conclusion

We calculate the binding energy of an hydrogenic impurity in a multi-layer QD which consists of a spherical core coating with a spherical shell (potential barrier V_2) and embedded in a bulk material (potential barrier V_3). Our MLQD model can be reduced successfully to the case of single layer QD if we set V_2=V_3. The results for a single layer QD are consistent with previous results. Our calculation shows as the dot radius becomes very large, the binding energy of the MLQD approaches 1Ry and thus behaves like a single layer QD. However, as the dot radius approaches zero, the behavior of the impurity in the MLQD is very different from that in the single layer. In the single layer QD, the binding energy approaches 1Ry as the dot radius reduces to zero, and behaves just like a free hydrogen atom in the bulk material. While in the multi-layer QD, as the core radius reduces to zero, the binding energy approaches different limiting values from zero to 1Ry. The limiting value depends on the difference between the barrier height of the shell potential and bulk potential. It is found that the binding energy and the position of electron can be adjusted by varying the barrier heights of the shell potential and bulk potential.

5. Acknowledgment

This work was supported by Deh Yu College of Nursing and Management.

6. References

1. T. Fukui, S. Ando, and Y. Tokura Appl. Phys. Lett. **58**, 2018(1991).

2. H. Fang, R. Zeller, and P. J. Stiles Appl. Phys. Lett. **55**, 1433(1989).

3. T. P. Smith Ⅲ, K. Y. Lee, C. M. Knoedler, J. M. Hong, and D. P. Kern Phys. Rev. B **38**, 2172(1988).

4. M. A. Reed, J. N. Randall, R. J. Aggarwal, R. J. Matyi, T. M. Moore, and A. E. Wetsel Phys. Rev. Lett. **60**, 535(1988).

5. Q. Ye, R. Tsu, and E. H. Hicollian Phys. Rev. B **44**, 1806(1991).

6. G. Bastard, Phys. Rev. B **24**, 4714(1981).

7. N. P. Montenegro, J. Lopez-Gondar, and L. E. Oliveira Phys. Rev. B **43**, 1824 (1991).

8. W. T. Masselink, Y. C. Chang, and H. Morkoc Phys. Rev. B **28**, 7373(1983).

9. J. W. Brown and H. N. Spector, J. Appl. Phys. **59**, 1179(1986).

10. G. W. Bryant Phys. Rev. B **31**, 7812(1985).

11. G. W. Bryant Phys. Rev. B **29**, 6632(1984).

12. R. C. Miller, A. C. Gossard, W. T. Tsang, and O. Munteanu, Phys. Rev. B **29**, 3871 (1982).

13. S. V. Branis, G. Li, and K. K. Bajaj Phys. Rev. B **47**, 1316(1993).

14. D. S. Chuu, C. M. Hsiao, and W. N. Mei Phys. Rev. B **46**, 3898(1992).

15. C. M. Hsiao, W. N. Mei, and D. S. Chuu, Solid State Commun. **81**, 807(1992).

16. S. V. Nair, L. M. Ramaniah, and K. C. Rustagi Phys. Rev. B **45**, 5969(1992).

17. G. T. Einevoll and Y. C. Chang Phys. Rev. B **40**, 9683(1989).

18. A. Kumar, S. E. Laux, and F. Stern Phys. Rev. B **42**, 5166(1990).

19. N. Porras-Montenegro, and S. T. P-Merchancano Phys. Rev. B **46**, 9780(1992)

20. J. L. Zhu, J. H. Zhao, W. H. Duan and B. L. Gu, Phys. Rev. B **46**, 7546(1992).

21. J. L. Zhu, J. J. Xiong, and B. L. Gu Phys. Rev. B **41**, 6001(1990).

22. J. L. Zhu and X. Chen Phys. Rev. B **50**, 4497(1994).

23. X. F. He, Phys. Rev. B **43**, 2063(1991).

24. K. Kash, A. Scherer, J. M. Worlock, H. G. Graighead, and M. C. Tamargo, Appl. Phys. Lett. **49**, 1043(1986).

25. B. J. Skromme, R. Bhat, and M. A. Koza, Solid State Comm. **66**, 543(1988).

26. H. Temkin, G. J. Dolan, M. B. Panish, and S. N. G. Chu, Appl. Phys. Lett. **50**, 413 (1987).

27. B. V. Shanabrook, J. Comas, T. A. Perry, and R. Merlin, Phys. Rev. B **29**, 7096 (1984).

28. D. Gammon, R. Merlin, W. T. Maselink, and H. Morkoc, Phys. Rev. B **33**, 2919 (1986).

29. S. Chaudhuri, Phys. Rev. B **28**, 4480(1983).

30. P. Lane and R. L. Greene, Phys. Rev. B **33**, 5871(1986).

31. D. Schooss, A. Mews, A, Eychmuller and H. Weller, Phys. Rev. B **49**, 17072 (1994).

32. A. Eychuller, A. Mews, and H. weller, Chem. Phys. Lett. **208**, 59(1993).

33. A. Mews, A. Eychuller, M. Giersig, D. Schooss, and H. weller, J. Phys. Chem. **98**, 934(1994).

34. A. Mews, A. V. Kadavaich, U. Banin, and A. P. Alivisatos, Phys. Rev. B **53**, R13242 (1996).

35. J. Kido, K. Hongawa, K. Okuyama, and K. Nagai, Appl. Phys. Lett. **63**, 2627 (1993).

36. B. Hu, Z. Yang, and F. E. Karasz, J. Appl. Phys. **76**, 2419(1994).

37. B. O. Dabbousi and M. G. Bawendi, O. Onitsuka, and M. F. Rubner, Appl. Phys. Lett. **66**, 1316(1995).

38. R. Tsu and D. Babic Appl. Phys. Lett. **64**, 1806(1994).

39. M. Lannoo, C. Delerue and G. Allan Phys. Rev. Lett. **74**, 3415(1995).

40. C. R. Proetto, Phys. Rev. Lett. **76**, 2824(1996).

41. S. Adachi, J. Appl. Phys. **58**, R1(1985).

42. A. Jeffrey, I. Ryzhik, I. Gradshteyn, Yu. Geronimus, and M. Tseytlin Table of Integrals, Series, and Products (Academic Press, New York, 1980) p. 1059.

43. G. Arfken Mathematical Methods for Physicists second edition (Academic Press, New York, 1973) p. 639.

44. A. Abramowitz and I. A. Stegun Handbook of Mathematical Function with Formulas, Graphs, and Mathematical Tables, Natl. Bur. Stand. Appl. Math. Series No. 55 (U. S. GPO, Washington, D. C., 1964) p. 538.